Slip Ring Electrical Anomalies Found After Protoflight Vibration Testing

Troy Nilson*, Scott Christiansen* and Chad Hebert*

Abstract

Following protoflight component testing of a Solar Array Drive Assembly (SADA), post-test electrical measurements revealed shorted circuits caused by slip ring brush displacement. Initial investigation, disassembly and analysis suggested the root case was related to insufficient preload in an axial bias spring constraining the slip ring rotor. Successful rework and re-test supported this conclusion. However, later tests of similar hardware for a subsequent program resulted in a comparable electrical anomaly. Original investigation results were reviewed and found to still be valid. However, additional contributing factors were identified that led to the reoccurrence of the anomaly. This paper explores the discovery, investigation, analytical approach, and ultimate resolution of a SADA slip ring anomaly.

Introduction

Over the past ten years, Sierra Nevada Corporation's (SNC) Space Systems group has designed, built and successfully flown a highly reliable and robust SADA (Figure 1) capable of transferring several kilowatts across a structurally integrated rotating interface connecting large solar arrays to spacecraft.

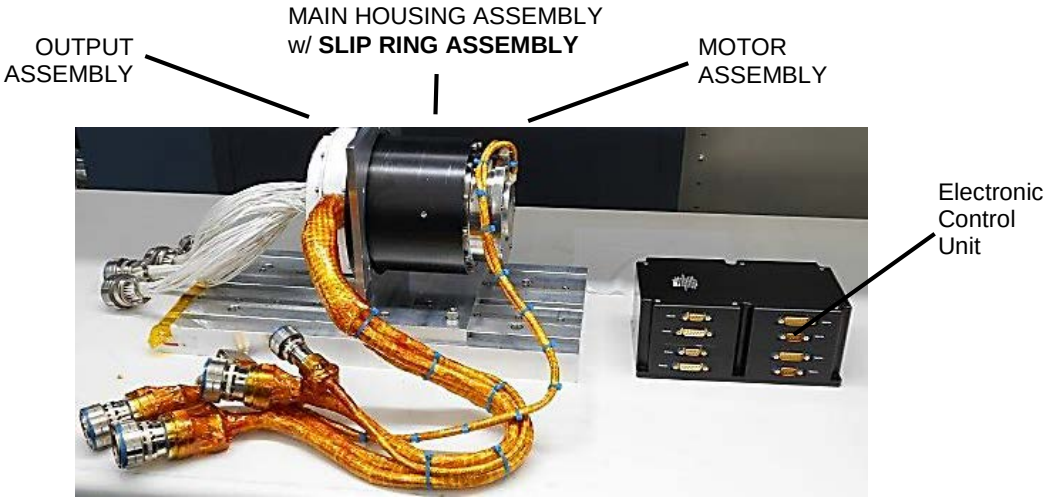

Figure 1. SADA System w/ Electronic Control Unit

Commonly experienced with high-reliability, low-volume production, the path to accomplishing this success has been achieved through desire for quality and focused efforts while working through design and test challenges. These challenges guided SNC through a series of events that allowed the engineering team to develop a highly refined SADA design and design process that optimizes the use of analysis tools such as high-fidelity Finite Element Modeling (FEM) to ensure design success. This paper explores the discovery, investigation, analytical approach and ultimate resolution of a SADA slip ring anomaly.

* Sierra Nevada Corporation, Louisville, CO

Environments and Hardware Description

To help understand the nature and subtle nuances of the SADA slip ring anomaly, it is necessary to understand required operational and test environments as well as discuss the various SADA subcomponents and related design goals. SNC was contracted to develop an electromechanical rotary device (and related Electronic Control Unit) designed to structurally support and rotate a greater than 20 kg-m^2 inertia payload (i.e., large solar array panel). The design was required to survive a 7-year mission in a high-vacuum space environment with thermal extremes ranging from -30ºC to +70ºC. Of particular interest to this discussion, the SADA was also required to withstand structural loading associated with random vibration testing and endure a thermal vacuum life cycle test of more than eighty thousand rotational cycles without slip ring electrical degradation or other electromechanical failure. Examples of the test setup, configuration, and levels are shown in Figure 2 and Figure 3,

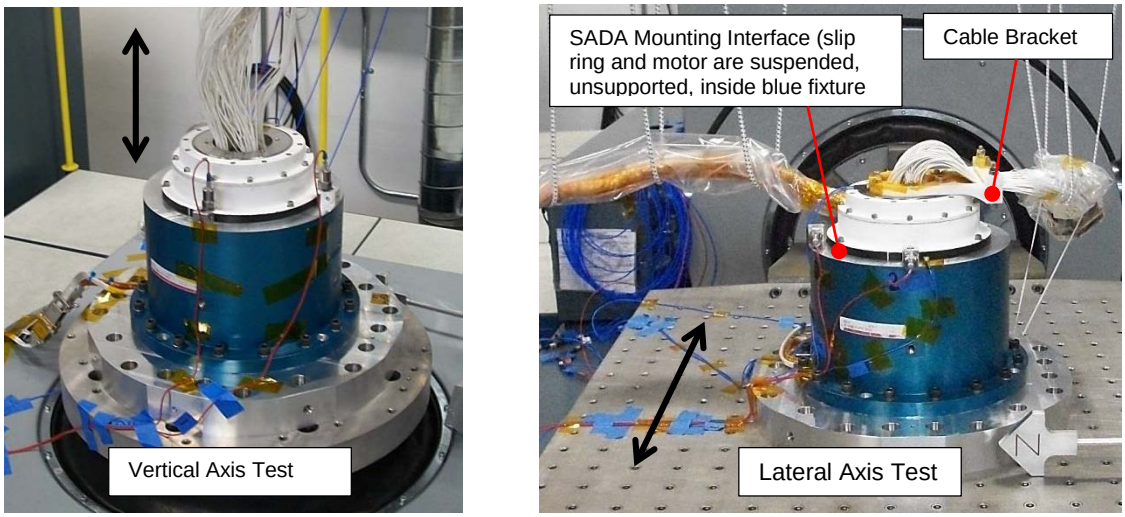

Figure 2. Photos of SADA Hardware Setup for Vibration Testing

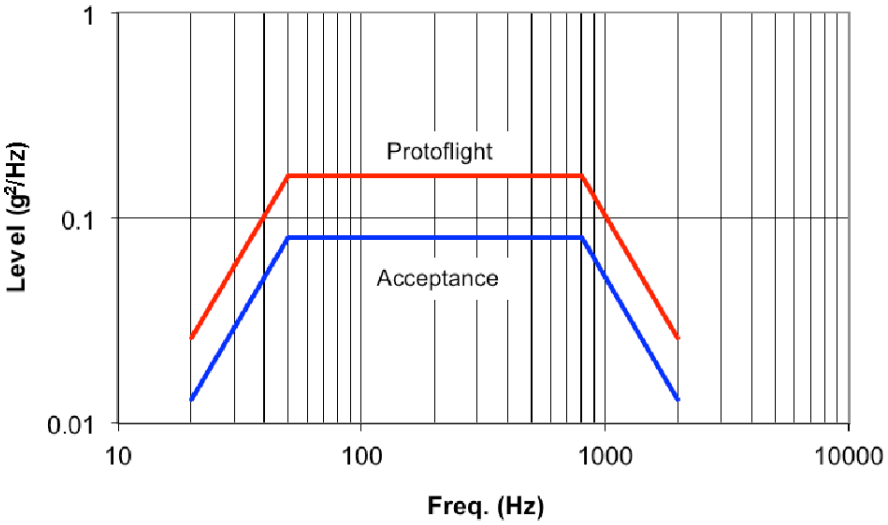

Figure 3. Specified Vibration Test Spectrum

At first glance, the noted g-levels do not appear to be unusual or exceedingly difficult design requirements. Standard design practices pre-anomaly were to ensure design integrity with positive margins up to 3-sigma peak acceleration loads. However, later evidence demonstrated this protoflight test profile, when applied to the SADA mounted in a very stiff test fixture, combined to produce SADA resonant modes that resulted in unexpectedly high (i.e., statistically low probability) input loads. In fact, resonant modes were later discovered to excite SADA components to as high as 2 to 3 times the control Grms input level. Additionally, these high responses contained greater than 6-sigma peaks during component vibration tests.

The SADA, illustrated in Figure 1, consists of four main subassemblies including the output, main housing, slip ring, and motor. The output assembly has a payload attachment interface that incorporates a set of duplex bearings designed to carry radial, axial and moment loads of the attached payload. The slip ring assembly shown in Figure 4 and Figure 5 consists of four brush block assemblies each with a series of gold alloy wires (i.e., brushes) supported and attached to printed circuit boards. Each brush rides in individual v-grooves machined into the slip ring rotor and each circuit/set of ring grooves (1 to 5 grooves per group) is physically and electrically insulated from each other with a raised insulation barrier as shown in Figure 5. This slip ring assembly is supported between the output assembly and another set of trailing bearings within the main housing assembly. At the opposite end of the SADA, away from the output assembly, the geared stepper motor is mechanically grounded to the main housing assembly and coupled to the output assembly torque transfer shaft passing through a clearance hole in the slip ring rotor. The completed assembly weighs approximately 12 kg and measures approximately 20-cm outer diameter by 23-cm long.

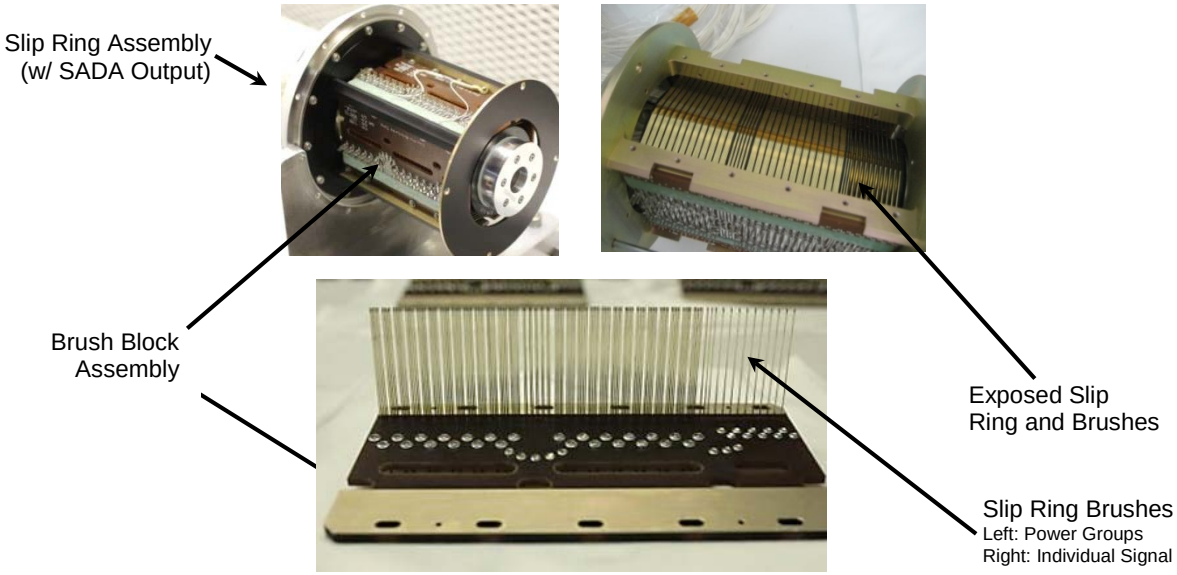

Figure 4. Slip Ring Assembly w/ Exposed Rotor and Brushes

This configuration incorporates several competing design objectives including meeting requirements to support very high moment and axial loads between the SADA mounting flange and the solar array attachment point while outputting very high stiffness as well as minimizing output drag to address a low disturbance torque performance requirement. The solution was to incorporate a high-precision, moderately-preloaded duplex bearing mounted as close to the payload as possible. These trades lead to a cantilevered design optimized for launch and on-orbit mission requirements but less desirable for component-level vibration tests and related SADA test boundary conditions.

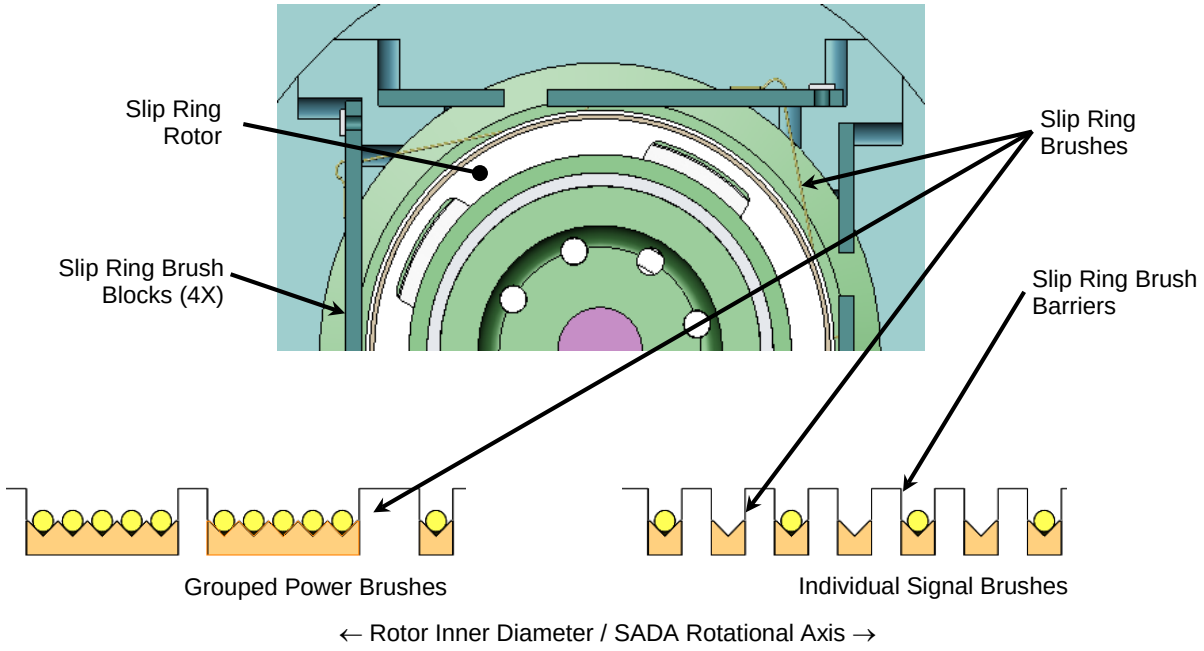

Figure 5. Illustration Slip Ring Rotor Ring Grooves and Brush Orientation

Other competing design goals central to the SADA slip ring design are related to brush preload. The relatively high cycle life requirement was best achieved through lightly preloaded brushes where lower forces would result in less drag and less wear at the contact point between the slip ring brushes and the rotor. Reduced brush drag and wear increases drive torque margins and decreases debris generation within the mechanism. Efforts to limit debris generation over time minimized contamination risk to other mechanical components within the SADA (such as bearings) and helped lower brush electrical stick/slip noise by allowing the brushes to remain solidly in contact with and electrically bonded to the slip ring rotor.

In contrast, the requirement to sustain random vibration loads was better addressed through higher brush preload. Higher preload provided increased margin against brush/rotor gapping during vibration testing and increased chances that the brushes would remain in assigned groves, keeping them isolated from neighboring rings to prevent unacceptable short circuits. Increased brush preload also minimized brush contact resistance and sliding contact noise.

While these competing design goals were challenging, SNC optimized the design, balanced these competing requirements and ultimately developed and manufactured a highly reliable and viable mechanism. The design has been integrated into several spacecraft and has several years of on-orbit mission success despite various challenges related to a short circuit anomaly that occurred during component-level testing.

Anomaly Discovery

During a standard post-test electrical check after a typical random vibration protoflight test of a newly developed and built SADA, SNC encountered the first of two key events associated with the slip ring short circuit anomaly. An electrical circuit isolation test confirmed several slip ring circuits had shorted together. Following this discovery, various other post-test functional checks were performed. The successful completion of these performance tests confirmed the SADA had no physical damage to any other components and, aside from the electrical anomaly, was operating as expected.

Through extensive design and data review, analysis, and disassembly of the SADA, SNC confirmed a random selection of slip ring brushes had 'jumped' across the rotor electrical insulation barrier and moved from assigned rotor grooves to neighboring grooves. The result was an anomalous ring-ring short circuit that caused the isolation test fault. Figure 6 shows a 3D radiographic image of displaced and shorted signal brushes.

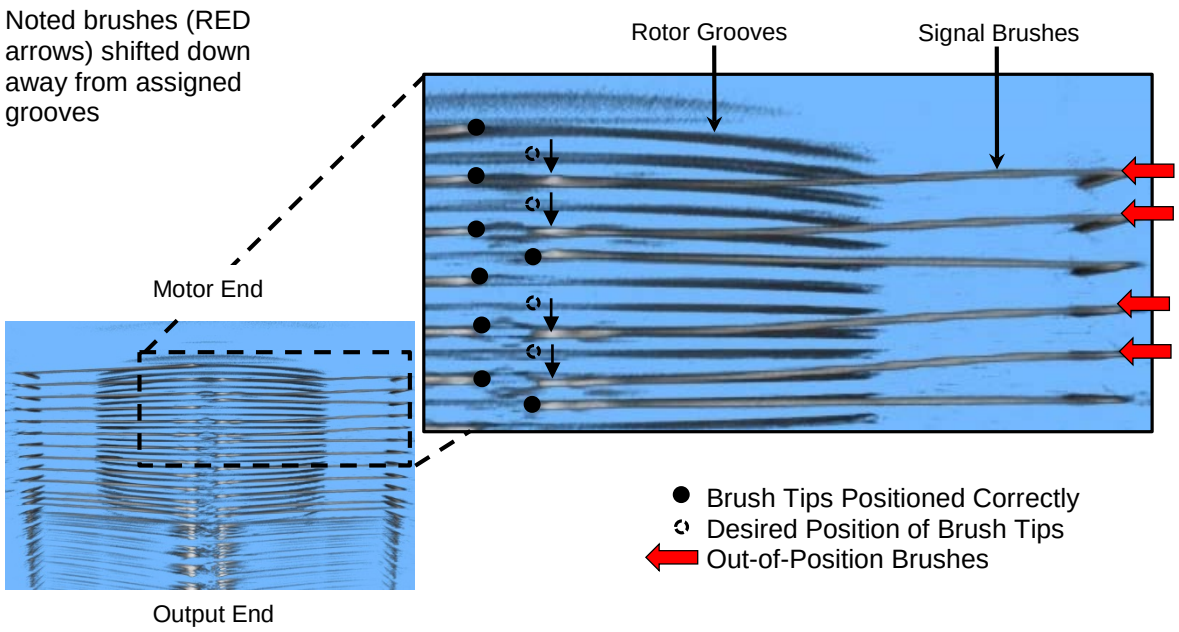

Figure 6. Radiographic Image of SADA Slip Ring with 4 Shorted Signal Brushes

This image was derived from 3D X-ray imaging processes and techniques not commonly available at the time of the initial investigation. However, the image is presented here because it clearly illustrates the condition of the brushes in a similar short circuit condition. Signal brushes are shown misaligned with the slip ring rotor grooves as they appear axially along the slip ring rotor. The right side bottom view of Figure 5 is a sketch of the desired alternating pattern for signal brush position. Four signal brushes shown in Figure 6 do not follow this pattern, (RED arrows) indicating movement away from their assigned grooves and causing a short circuit between adjacent rings.

Due to the enclosed configuration of the SADA, visual confirmation of the slip ring rotor and brush condition was not feasible. Prior to the application of this 3D X-ray imaging technology, other methods such as standard electrical isolation tests and resistance measurements were used to confirm the initial slip ring fault. Electrical isolation test results allowed the team to adequately identify the precise circuits involved but they did not provide enough data to confirm which brush moved to which ring. To collect the additional data required, the team utilized high-fidelity resistance measurements of each identified anomalous slip ring circuit pair. By comparing measured parallel resistance to historical values, the circuit with the displaced brush(es) could be identified by higher than expected resistance readings.

After testing was conducted to identify the presence of the displaced brushes, it was found through further data review and analysis that the slip ring rotor preload spring force was not providing enough holding force to axially stabilize the rotor during random vibration testing. The investigation team believed this insufficient rotor preload allowed the rotor to "gap" and axially oscillate during test. These oscillations resulted in very high undamped impact loads each time the rotor re-seated against internal axial hardstops. This rotor impact imparted forces into brushes beyond established preload that, when combined with resulting complex nonlinear brush dynamics, caused the brushes to break contact with the

slip ring rotor and move onto adjacent circuits. This hypothesis was confirmed with a successful random vibration re-test following SADA rework by repositioning the brushes to their assigned grooves and increasing the rotor axial preload to withstand higher-than-expected rotor acceleration responses.

Several years later, after two successful SADA on-orbit missions, protoflight vibration testing once again resulted in shorted slip ring circuits. Because of historical issues with slip ring rotor preload, initial discovery efforts focused on the as-built condition of new hardware and found rotor preload to be slightly underrated. However, subsequent rework to correct rotor preload did not prevent brush movement during vibration re-tests. It became evident that underrated rotor preload was not the only physical cause for the anomaly and SNC began a rigorous in-depth investigation to reevaluate other underlying causes.

Anomaly Investigation

Dealing with problems associated with the structural response of complex mechanical systems can be extremely challenging, especially when investigation and discovery must be conducted on fully assembled flight hardware with limited visibility or access to key components. This 'black box' scenario once again became the backdrop for another rigorous investigation into the root cause analysis of the shorted brushes.

The investigation centered on three key areas including review of design/analysis/build documentation, assessment of dynamic responses on various SADA components, and development of test correlated predictive analytical tools. First, an extensive review of build documentation found the SADA parts to be correctly manufactured and assembled to print. Review of various structural analysis reports confirmed positive load margins. All evidence, additionally supported by rigorous visual inspections during hardware disassembly, convinced the engineering team that the anomaly did not occur as a result of a failed or incorrectly assembled component. No obvious root cause explanation was found, so the team focused on the second area of interest, dynamic response, which quickly became the primary focus of the investigation.

The team shifted the investigation focus to data mining, including exhaustive efforts to collect, evaluate, and categorize prior SADA acceptance test data. The effort began with a rigorous study of accelerometer output time history in an attempt to further quantify the frequency and nature of peak input loads. Data consisted of several vibration tests and re-tests of similar SADA hardware, test setup, and vibration input profiles conducted throughout a ten-year period.

Time history vibration data revealed that unexpected intermittent responses greater than 6 sigma were present during test, including tests that resulted in shorted slip ring circuits. Figure 7 illustrates an example of a time history plot recorded during a prior SADA vibration test. This finding was crucial to the investigation because it confirmed that the typical 3-sigma threshold used for design and analysis was inadequate for the design of this particular component as tested under the specified vibration spectrum and related test boundary conditions. Review of this data provided a comprehensive understanding of vibration test effects on and interaction with the SADA that contributed to the team's ability to develop a viable method of predicting dynamic response during future tests.

Discovery of these random peak loads was a critical breakthrough in the investigation. It became immediately clear that prior design efforts did not account for these significantly higher dynamic events. The persistence of these higher events in historical data highlighted a need to increase the previous minimum design standard from 3 to 6 sigma or greater for this particular component and to begin work on the development of higher fidelity predictive modeling techniques.

As the effort to develop predictive modeling techniques began, it became apparent that trying to quantify and predict the dynamic behavior and movement of hundreds of independent brushes reacting against the slip ring rotor would be very challenging. However, the team realized that it was not necessary to fully understand or predict the complex nonlinear behavior of brush dynamics. Instead, the engineering team

developed an analytical method to predict the load at which a brush would gap ('lift-off') away from the rotor. The underlying theory was that a brush that does not gap cannot inadvertently displace to adjacent slip ring circuits. The plan was to compare the recovered brush tip reaction loads to the as-built brush preload and establish margins against gapping. With this approach in mind, efforts shifted to predicting gapping events rather than trying to understand complexities of brush dynamics once gapped. Finite element analyses became the focus in this next phase of the investigation with the primary goal to refine and test-correlate an existing SADA finite element model (FEM) and develop a high-fidelity predictive tool.

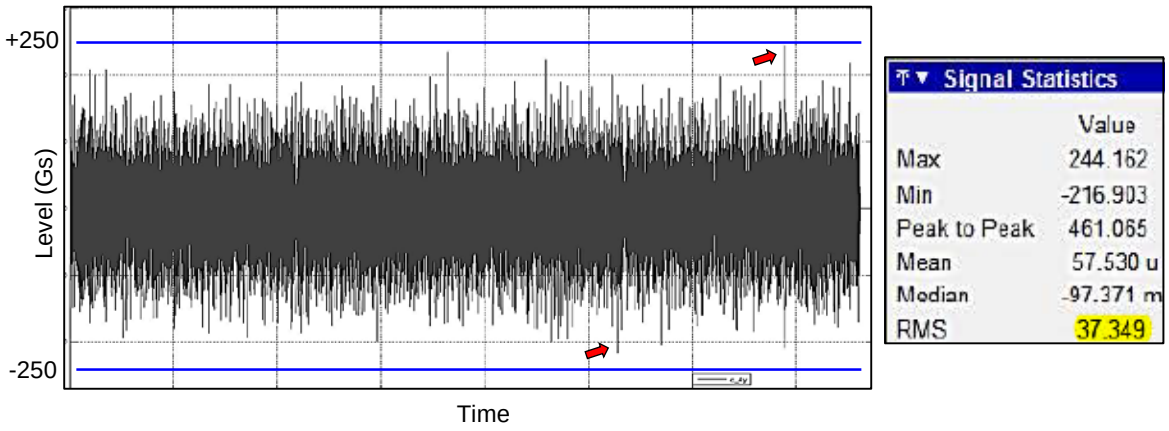

Figure 7. Accelerometer Response Data - Time History Recorded During Vibration Testing

This process to refine the existing SADA FEM started with a fundamental update to incorporate individual brushes around and along the slip ring rotor. Several power ring brush groups as well as a series of single signal brushes were placed in strategic locations including areas where known short circuit events had occurred. Each brush was modeled to closely match the shape, cross-sectional geometry, and mechanical properties of the brushes used. Most importantly, these brushes were restrained at the contact points between the brush tip and rotor. The purpose of these FEM updates was to devise a method of recovering brush/rotor reaction loads that could be then be compared to as-built brush preload. This comparison could then be used to establish gapping margin estimates for SADA exposure to various input spectrum and random vibration test conditions. With this goal to accurately predict the 'lift-off' threshold, further FEM development and refinements continued.

The next phase of this FEM development involved test-correlating the analytical model to the as-built hardware. The process began with comparison of FEM results to prior test data. Comparison confirmed that the refined model was closely predicting the SADA response, but two issues surfaced and complicated the task of further FEM refinement. First, prior data review and data mining efforts found minor variations in test setup, SADA design, and boundary constraints associated with the various tests. These minor test and hardware configuration differences were not unexpected given the progressive development of the SADA spanning several years and following many different test programs, each with its unique assembly and test history. Variables included minor differences in cable bundle boundary constraints, rotational alignment, rotor axial preload, brush contact preload, accelerometer placement, and vibration test equipment/facilities. Table 1 summarizes some of these configuration differences. Because the historical data sets were complicated by these differences, precise tailored FEM correlation was extremely challenging and it became clear that additional test data would be required to continue the FEM model-correlation and refinement effort.

Table 1. Example of Various Hardware Test Configurations

Output Fiducial Alignment	Diving board orientation RE: Table X axis	Diving board orientation RE: Table Y axis	Diving board orientation RE: Table Z axis	Diving board orientation RE: Case Fiducial	Should be: Diving board orientation RE: Case Fiducial	Bus wire exit X axis	Bus wire exit Y Axis	Bus wire exit Z axis
-60°	N/A	N/A	N/A	N/A	-105°	Back Left	Back Left	Front Left
-60° to -120°	Right	Right	Back	-105°	-105°	Back Left	Back Left	Front Left
+86°	Back	Back	Left	+165°	+75°	Back Left	Back Left	Front Left
Aligned	Left	N/A	Front	+75°	+75°	Back Left	N/A	Front Left

Note: Use of the term 'diving board' is synonymous with output cable bundle and clamp

The second issue with the historical data involved accelerometer placement and related availability of response data. Standard vibration tests include application of strategically placed accelerometers on the exterior SADA surfaces and surrounding test fixtures to recover selected mechanism dynamic responses during test; this placement on the exterior is typical. Other more sensitive components are housed within an enclosed structure to protect them from contamination and handling prior to launch. These sensitive components are very seldom accessible, making instrumentation and recovery of dynamic response difficult. Because this short circuit anomaly involved dynamics of sensitive internal SADA components, the lack of sensors and response data nearer to the brushes raised concerns regarding FEM correlation accuracy.

To address these two challenges, a tailored low-level vibration test (-6 dB) was conducted on flight hardware reworked to as-designed configuration (i.e., verified slip ring rotor preload and properly repositioned and aligned brushes). The test article was instrumented with strategically placed accelerometers consistent with the orientation and position defined in protoflight test setup documentation and found during data review of historical tests with one exception. One additional accelerometer was temporarily installed deep inside the SADA on the slip ring rotor shaft. This additional sensor was critical to SNC's understanding of the SADA response within the mechanism nearer to the brushes. Test results were then used to further refine the FEM and complete the development of this test-correlated predictive tool to within 1% of measured values.

Figure 8 illustrates an example of results from a lateral (z-axis) low-level random vibration test compared to simulated output of the refined FEM. As shown, the peak level and resonant frequency of the rotor shaft for both the test and predictive model align very closely around 650 Hz, which indicates a highly refined FEM model. All remaining axes were test correlated in a similar manner to complete the effort. Armed with a newly-developed, high-fidelity test correlated FEM, SNC was able to analyze earlier anomalous tests and confirm low brush force margins when tested to the specified levels. FEM model predictions using baseline protoflight test levels shown in Figure 3 confirmed that the slip ring rotor shaft modes closely aligned with the SADA primary structural modes. Resonance at this aligned frequency significantly increased the likelihood of very high peaks (6 sigma and greater) and explained higher-than-expected brush contact point response loads. Figure 9 illustrates the first mode of the SADA structure at the far end of the cantilevered assembly (i.e., motor end) aligned with data collected on the interior of the SADA at the end of the slip ring rotor shaft nearest the brushes that shorted. Analysis results confirm that when tested to the required protoflight vibration levels while constrained in test fixtures as defined in related protoflight test procedures, brushes would exceed preload and gap with as little as 3.8-sigma events. And as discussed earlier, greater than 6-sigma events were not uncommon. This finding clearly supports the statement of cause noted below.

Primary Physical Cause: *Protoflight testing to specified vibration levels induced loads into SADA and related slip ring brushes sufficient to overcome brush preload and force brushes to adjacent slip ring circuits. This condition resulted in ring-ring short circuit.*

Root Cause: *Required protoflight random vibration test levels and associated test boundary conditions uncharacteristic of flight environments created response loads that exceeded the design capability of the SADA brush configuration.*

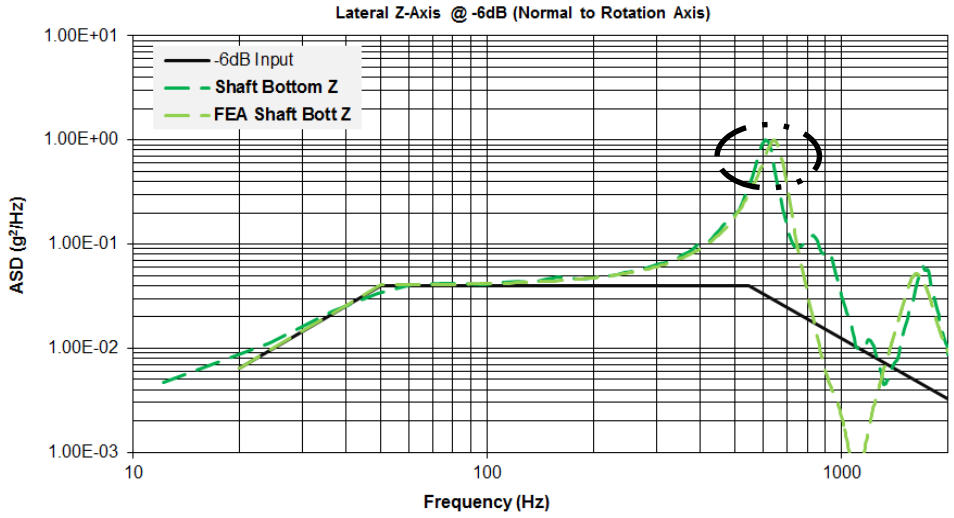

Figure 8. Data plot of test correlated FEM for lateral Z-axis response

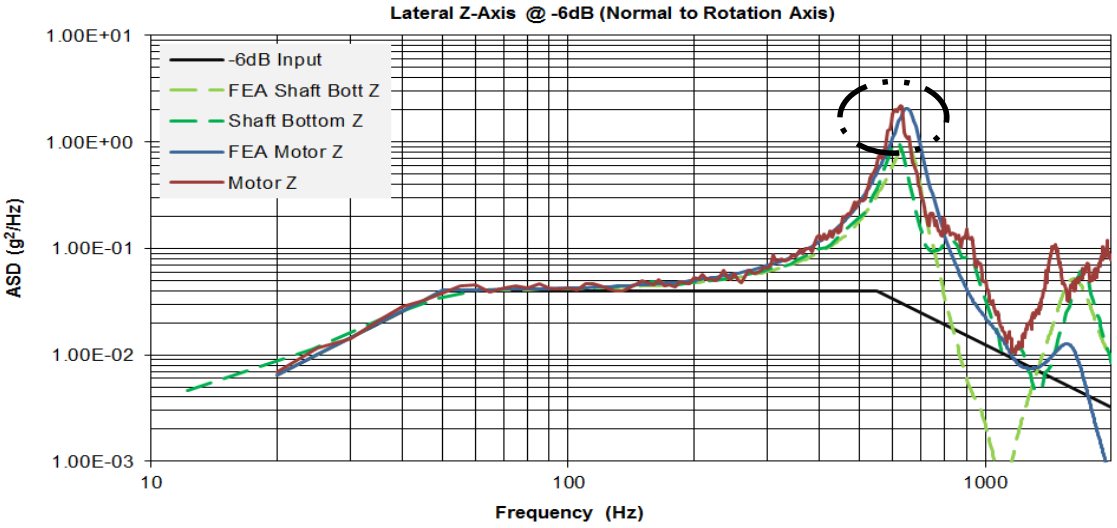

Figure 9. Data Illustrating SADA Primary Structural Modes Aligned with Rotor Shaft Modes

Anomaly Resolution

The engineering team initially considered various options to physically modify the SADA design and address the likely recurrence of shorted brushes. Analysis efforts began to assess whether-or-not modifications to stiffen primary structural parts of the SADA (i.e., housings, supports, etc.) would help shift and separate the SADA primary structural mode from the peak brush mode. Without significant impacts to the SADA envelope and mass, FEM analysis results confirmed this was not a viable option. The team

also considered improvements to mechanically constrain brushes to keep them within assigned rings and below insulation barriers. This modification could either be implemented with a deployable launch lock configuration or by snubbing brushes to limit stroke once installed and assembled in their assigned grooves. However, associated design changes would have required significant development effort and included an array of additional technical risks. Cost and schedule constraints combined with related technical risks ultimately made the feasibility of fundamental design changes to fully assembled and qualified hardware in the middle of final acceptance testing very undesirable.

Without making physical changes to the SADA, the only other viable options were to either re-evaluate and modify test boundary conditions to more accurately represent spacecraft test and launch environments or tailor the random vibration test profile (via force limiting, notching, and/or other profile changes) to limit input loads to reasonably margined levels. To address the first potential solution, the team further reviewed spacecraft test and launch data and confirmed that the required component test levels combined with the rigid SADA/fixture boundary conditions resulted in very different SADA input loads. Review found SADA component level test loads were significantly higher than any loads measured at the SADA when integrated with the payload and mounted to the spacecraft. In addition, data also revealed that the majority of energy input into the SADA during launch and spacecraft level tests occurred well below the SADA resonant frequency of 650 Hz. These findings confirmed beliefs that component tests resulted in SADA loads far above of levels needed to demonstrate compliance with launch and spacecraft test environments.

It is well known that accurate physical simulation of launch/interface boundary conditions at the component level is extremely difficult and complex and the team believed that attempts to lower SADA input loads by changing test boundary conditions would be very risky. Any change would significantly lower the team's understanding and certainty related to SADA response during test and the value of a known response far outweighed the risks of uncertainty. Major design changes to the SADA test boundary conditions were not implemented. However, one minor change was feasible.

To more accurately match cable bundle loads and related SADA rotor shaft dynamic response during test, a minor change to the SADA test boundary conditions was implemented. This involved modifications to the output cable bundle support and clamping method. Brackets were manufactured and installed on the SADA to more accurately represent the as-integrated SADA/spacecraft configuration. FEM analysis confirmed the change would improve margins, and any easily-implemented change for the better with relatively low impact to program cost and schedule made sense. This configuration difference can be seen in Figure 2 where the installation of a cable clamp is shown in the image on the right.

Because major changes to boundary conditions were not feasible, the team changed focus to solutions that involved vibration test profile modifications. Because early test instrumentation did not include an accelerometer at the cantilevered end (i.e., motor end) of the SADA, review of available test data identified the SADA primary structural mode related to brush movement to be an axial mode near 800 Hz. The protoflight profile (Figure 3) coincidentally included a plateau out to 800 Hz. The team believed excessive loads on the rotor high enough to cause brush movement could be minimized by decreasing the test profile roll-off point from 800 Hz to 550 Hz. Re-tests to this modified profile did not solve the problem and related slip ring short circuit conditions persisted. This indicated that the initial understanding of the brush movement was incomplete.

It is important to note that at the time of this 550-Hz modified profile testing, development of a high-fidelity FEM model was incomplete. In fact, it was the recurrence of the short circuit anomaly following the 550-Hz test that caused an aggressive shift in the investigation and ultimately lead to the discovery of the 650-Hz lateral mode discussed earlier.

Rather than continuing to resolve the problem by marginally changing test spectrum profiles, output from the new high-fidelity FEM model was used to justify the application of more rigorous test techniques and manage excessive SADA responses. Vibration test profile-notching and force-limiting were two

techniques considered. Ultimately, a plan was developed to utilize force-limiting to reduce peak loads at mechanism resonant frequencies. The Semi-Empirical method from NASA-HDBK_7004C ("*Force Limited Vibration Testing*") was the approach implemented. This test method uses load response data from force gauges placed at the component/fixture mounting interface for closed-loop feedback to the shaker control system. The goal was to modulate shaker input into the test article and reduce the overall PSD at select frequencies while maintaining a pre-determined force level at the input.

As discussed earlier, FEM simulation results from the refined model highlighted the SADA first lateral mode around 650 Hz. The refined model was used to run force-limited simulations to predict the effects of a deep notch in the shaker input around the SADA resonant frequency shown in Figure 10. Simulation results match data recovered from successful SADA re-tests. For reference, this result is compared to GEVS minimum workmanship levels.

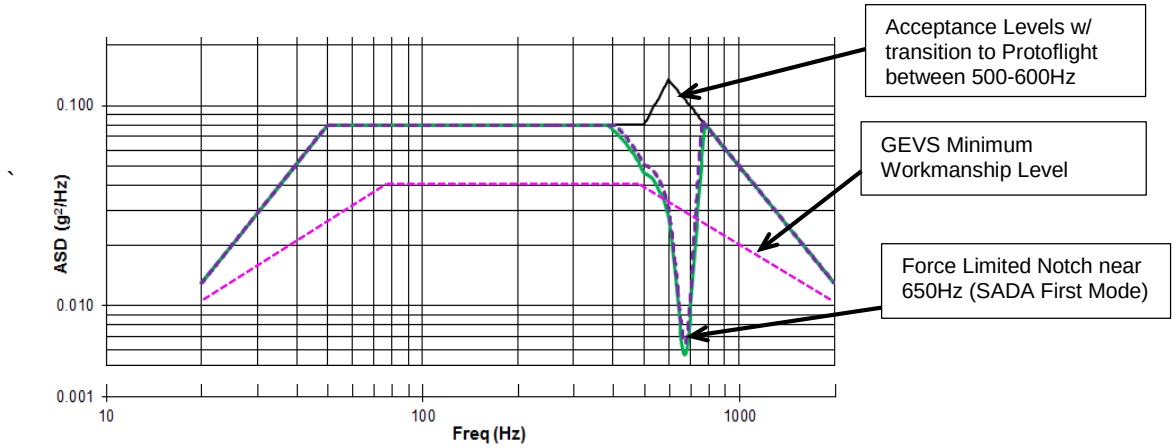

Figure 10. Profile Comparisons - Force Limiting FEM Predictions (Lateral Axis)

While this force-limited test method worked to address the immediate concerns of the ongoing program (i.e., the re-tested SADA did successfully survive the force-limited tests), the method is not preferred. The modified process and resulting profile did not adequately address the high brush loads at the second mode where as little as 3.2-sigma events could cause slip ring brushes to gap. Additionally, this type of testing is extremely time consuming and resource intensive. High-level engineering oversight by skilled dynamists prior to and during each run is required to ensure the control system and feedback process yield precisely correct test article input loads. Numerous low-level tests are required and run prior to each full-level test for each axis. With each run, response data must be scrutinized to verify that control set points are properly configured to achieve desired input response at full level. This intensive oversight and test complexity combined with the inherent risk and increased costs motivated the team to find a different approach to address the over-test problem for subsequent SADA tests.

Figure 11 is an example of key output from the improved test-correlated FEM and related analytical process. It shows the FEM prediction for brush force during the force-limited test shown in Figure 10 and clearly identifies both the first and second modes of the SADA that were believed to be responsible for the brush excitation during test. These results depict a peak brush/rotor contact load of 1.25 grams with contributions of 0.5 gram at SADA resonant frequencies up to 650 Hz and the remaining 0.75 gram at frequencies from 650 Hz up to the second mode near 1600 Hz. Results from simulations like these helped the team realize the importance of secondary resonant effects in any planned solution intended to mitigate brush movement during test. As the plot illustrates, energy in the brushes was significantly larger due to the second higher frequency peak. This was a very important finding that highlighted a need to seriously consider the impact of higher as well as lower frequency content when defining future test profiles.

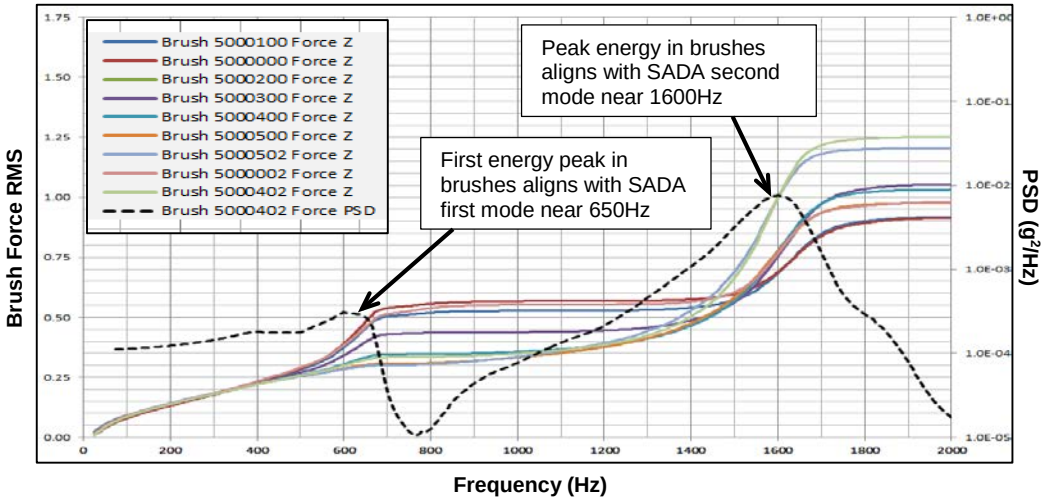

Figure 11**. Cumulative Brush Force (RMS) – Force Limiting FEM Predictions (Lateral Axis)**

The engineering team now had a nicely correlated FEM, a strong understanding of slip ring brush behavior, and recent experience with force-limited vibration test challenges. The desire for a new follow-on program was to utilize the FEM to analytically justify modification to existing vibration test requirements and ensure input levels remained well below brush gapping threshold of the exiting design. Several scenarios were evaluated during prior investigations while others were run to help assess new options and find a preferable compromise. Table 2 summarizes results from a few scenarios along with brush preload predictions. While analytical values do not quite achieve the gapping factor design goal of 6 sigma or greater, significant improvement can be seen in the gapping factor column.

This improvement was possible because brush gapping problems were well understood from prior investigations. This knowledge led to a slight but crucial change to the as-built brush preload that simply involved narrowing the preload tolerance window. Confidence that the as-built SADA included these higher preloads was gained by measuring brush preload at both the slip ring subassembly level and after integration with the SADA. This tolerance change resulted in a 25% increase over the minimum allowable brush preload previously specified, minimized the extent of random vibration profile tailoring required, and preserved the validity of the qualified SADA design. Implementation of this change left the remaining task of defining and justifying an acceptable random vibration test profile modification.

Table 2. Examples of FEM Brush Gapping Results with Margin Estimates

Random Vibe Environment	**FEM Brush Preload Prediction** (grams)			**Minimum Allowable Brush Preload** (grams)	**Gapping Factor** (σ)
	Z Axis (lateral)	X Axis (lateral)	Y Axis (axial)		**Z Axis** (lateral)
550 Hz roll-off, Protoflight (brushes shorted during test)	1.6	1.1	1.2	4.0 5.1*	2.5 3.2
550 Hz roll-off, Force Limit 30G (not tested)	1.2	1.0	0.9	4.0	3.3
350 Hz roll-off, Protoflight/GEVS (passed tests)	1.0	1.1	1.0	5.0 5.5*	5.0 5.5

*Measured sample average brush force

The prevailing opinion of design reviewers was that any modified profile needed to closely match the required protoflight level and deviations from these levels had to remain above component minimum workmanship standards to comply with accepted industry standards defined in NASA technical standard

GSFC-STD-7000 (General Environmental Verification Standard (GEVS)). Figure 12 compares the proposed test levels (i.e., Final Modified Profile, plot 4) with GEVS and other historical profiles. These comparisons highlight the strategic reduction in test input levels at frequencies greater than 350 Hz and contrasts the proposed profile to those associated with unsuccessful SADA tests.

The proposed test profile met most criteria and was ultimately approved by the review community. The 350-Hz roll-off was selected because it was safely under the approximate 650-Hz natural frequency of the SADA but well above (and inclusive of) significant response expected at the SADA during launch and spacecraft level tests. The profile also included a transition at 600 Hz from a straight to a kneed ramp. This transition kept the test levels above GEVS minimum workmanship requirements and mitigated concerns voiced during force-limiting tests when input significantly dropped below GEVS at the notched frequency (Figure 10).

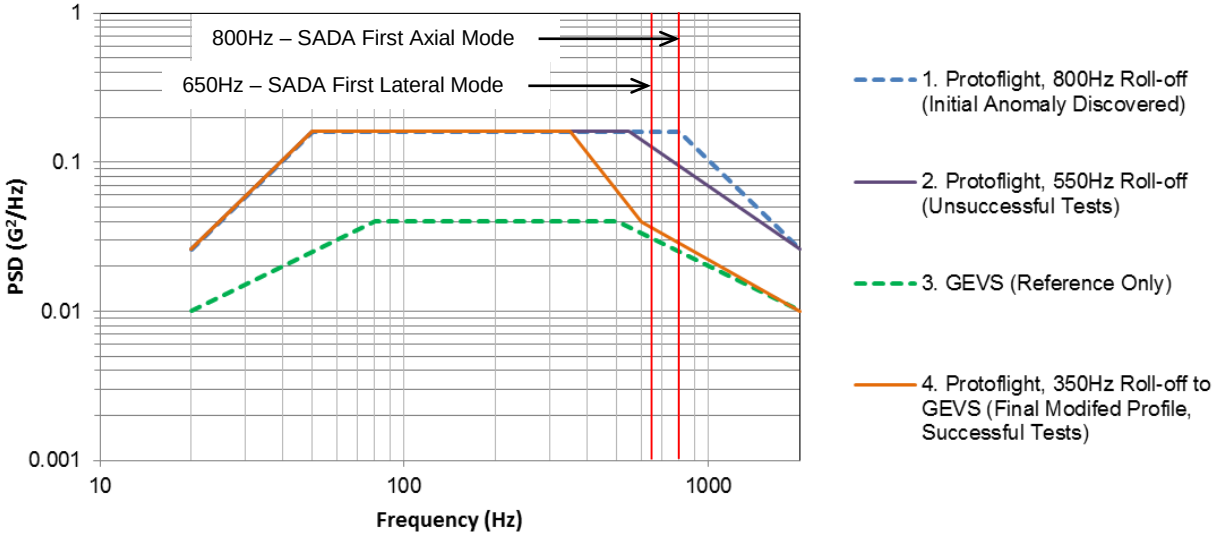

Figure 12. Final Tailored Vibration Profile Comparison

The final modified profile did fall slightly short of the design goal to demonstrate analytical margin against 6-sigma dynamic load events but the team felt the risk of gapping remained very low. Brush force margin against an estimated 5.5-sigma load event still represented a very low likelihood of occurrence and the design included additional inherent force margin against brush movement out and away from an assigned groove if brush gapping did occur. This modified profile was validated when SADAs built for the follow-on program passed all required protoflight testing, including slip ring electrical isolation and resistance checks, without issues. Review of post-test 3D radiographic brush block and rotor images similar to Figure 6 confirmed all brushes were properly aligned and positioned within assigned rotor grooves after exposure to the modified test profile.

Summary

The combination of increased minimum brush preload and testing to a modified random vibration test profile ultimately resulted in the successful completion of the SADA protoflight test program. This final success was a result of efforts from analysts, designers, and the entire review community starting with the discovery of the initial fault through to the successful delivery of several sets of hardware. During this process, significant insights were gained that will help mitigate the recurrence of similar problems in future designs.

Complex mechanical systems require a significant amount of scrutiny to ensure all fundamental frequencies are characterized and understood. This is especially true for systems that contain compliant structure housed in a very rigid primary structure. In the case of this SADA, the design guideline to evaluate dynamic loads against 3-sigma events for certain components seemed appropriate during the design and development phase. However, the investigation that followed the slip ring short circuit anomaly clearly identified a need to look beyond this 3-sigma guideline and apply a much higher standard, closer to 6 sigma. This need to increase load margins must be balanced with associated increased costs as well as other technical trades that may drive design complexity and technical risk.

During any design evaluation phase to consider whether-or-not increased load margins are required, test boundary conditions deserve a very critical review. Test boundary conditions can significantly impact technical trades and design decisions. Often, as seen in this case, component boundary conditions during protoflight or acceptance vibration testing rarely represent the as-integrated final flight configuration with the spacecraft. Understanding these differences and working to tailor test requirements prior to test to match component input levels (often at test specific resonant frequencies) can save countless investigation hours and wasted costs.

Familiarization with all forms of test and hardware evaluation technology is also beneficial. During this investigation, the team utilized complex force-limiting vibration test methods, high-fidelity test correlated FEMs, and advanced technology 3D radiographic imaging to resolve a very difficult technical challenge. However, the selection of applicable technology (new or old) is a far more important consideration than the use of new high-tech methods and equipment in general. For example, this investigation warranted the use of 3D imaging because the problem confirmation and re-test validation would have been significantly more difficult without it. This may not be true for future programs when reviewing new designs where alternatives to this technology, such as design modification to include view ports, may be more appropriate.

As with any complex problem, it is important to exhaustively consider alternatives, utilize technology appropriately, and support highly collative design experiences. In this case, SNC successfully did this to link high brush loads encountered during protoflight vibration testing to high SADA resonant peaks atypical of flight-like conditions. Findings from extensive data review, analysis, and design assessments highlight the need to thoroughly understand the impact of test boundary conditions and related mechanism resonant modes when designing complex mechanisms. Brush preload, beam shape and cross section, rotor support structure, and fundamental mechanism frequencies all interplay to present significant design and test challenges.

Despite the challenges faced during component level testing, SNC remains convinced that the SADA design is well suited to meet all mission requirements. To date, seven of these SADAs are successfully performing all required on-orbit operations and have accumulated more than 35 years of total operating time.